FULL PAPER

High-Performance Ferroelectric Memory Based on Phase-Separated Films of Polymer Blends

*Mohammad A. Khan, Unnat S. Bhansali, Mahmoud N. Almadhoun, Ihab N. Odeh, Dongkyu Cha, and Husam N. Alshareef**

High-performance polymer memory is fabricated using blends of ferroelectric poly(vinylidene-fluoride-trifluoroethylene) (P(VDF-TrFE)) and highly insulating poly(p-phenylene oxide) (PPO). The blend films spontaneously phase separate into amorphous PPO nanospheres embedded in a semicrystalline P(VDF-TrFE) matrix. Using low molecular weight PPO with high miscibility in a common solvent, i.e., methyl ethyl ketone, blend films are spin cast with extremely low roughness (R_{rms} ≈ 4.92 nm) and achieve nanoscale phase seperation (PPO domain size < 200 nm). These blend devices display highly improved ferroelectric and dielectric performance with low dielectric losses (<0.2 up to 1 MHz), enhanced thermal stability (up to ≈353 K), excellent fatigue endurance (80% retention after 10^6 cycles at 1 KHz) and high dielectric breakdown fields (≈360 MV/m).

1. Introduction

Flexible electronics research has made tremendous progress during the past 15 years, specifically in the area of organic thin film transistors (OTFTs), organic light emitting diodes OLEDs) and sensors. An integral part of any flexible electronic circuits is a non-volatile memory component that can be used to store and retrieve information as required. Polymer memories continue to be the biggest hurdle in the development of polymer-based flexible electronics. Among polymer memories, ferroelectric memories based on P(VDF-TrFE) are one of the leading candidates in the flexible and organic electronics community due to its easy low-temperature processability, excellent chemical stability, sufficiently large spontaneous polarization, non-volatility, and short switching times.[1,2]

The potential of polymer ferroelectric memory was realized more than two decades ago but has not lead to any major commercial products. Some of the important limitations include poor leakage, high surface roughness, poor thermal stability, poor fatigue/retention endurance and low breakdown strength of thin film P(VDF-TrFE) ferroelectric memory devices.[1] In particular, the poor thermal stability and poor fatigue performance of the P(VDF-TrFE) thin films remains a major hurdle for commercialization of polymer ferroelectric memory.[1,3] In recent years there have been numerous studies on the effect of different electrodes and interlayers on charge injection and fatigue performance of ferroelectric memory.[4–6] Nonetheless fatigue continues to be a big issue when characterized at a frequency low enough at which the dipoles in the copolymer can switch and at an applied field close to saturation field of the ferroelectric thin film.[7,8] Furthermore there are very few limited studies on the issue of thermal stability and poor breakdown strength of thin film P(VDF-TrFE) ferroelectric capacitors.[9,10] In contrast to the strategy of modifying electrodes and interfaces to improve performance of polymer ferroelectric capacitors, one can look at modifying and optimizing the properties of ferroelectric thin films. One very promising and interesting approach is to blend ferroelectric polymers with low-k dielectrics to improve their properties. PVDF and P(VDF-TrFE) blend films have primarily been studied with PMMA which shows excellent solubility up to 40 wt%.[11] PVDF and PMMA blend systems have been studied, to observe effect of PMMA on the crystallization of PVDF and growth of nanocrystalline ferroelectric β phase in PVDF. These systems are complicated to fabricate as the blend films have to be melted, quenched in ice water and further annealed to get the desired ferroelectric properties.[10,12] P(VDF-TrFE) copolymer also has good miscibility with PMMA up to 40 wt%. Earlier studies have characterized the morphology, dielectric and ferroelectric properties of P(VDF-TrFE)/PMMA blends and shown an improvement in performance.[13–15] Apart from PMMA, there are almost no reports of P(VDF-TrFE) blends with other insulating polymers for ferroelectric memory applications.

In this study we report the fabrication of thin film ferroelectric capacitors using blends of P(VDF-TrFE) with PPO. PPO is an amorphous high performance polymer dielectric with excellent electrical properties (good insulator, low dielectric losses), high temperature stability, good chemical resistance, low moisture absorption, and high mechanical and dielectric strength.[16,17] To our knowledge this is the first exhaustive study of P(VDF-TrFE)-PPO blend system for ferroelectric memory applications. We characterize the morphology and nanoscale

M. A. Khan, Dr. U. S. Bhansali, Dr. D. Cha, Prof. H. N. Alshareef
King Abdullah University of Science and Technology (KAUST)
Thuwal, 23955–6900, Saudi Arabia
E-mail: husam.alshareef@kaust.edu.sa
M. N. Almadhoun, Dr. I. N. Odeh
SABIC Corporate Research and Innovation Center
Thuwal, 23955–6900, Saudi Arabia

DOI: 10.1002/adfm.201302056

phase separation of these blends using atomic force microscopy (AFM) and cross-section transmission electron microscopy (TEM) imaging. The crystallinity and inter-planar distance of polymer chains was evaluated using grazing incidence X-ray diffraction (GIXRD) while the bonding and dipole orientation was analyzed using Fourier-transform infrared spectroscopy. Furthermore, we report an exhaustive electrical and ferroelectric characterization of these blend films in a metal-insulator-metal (MIM) capacitor structure using polarization–voltage, current–voltage, dielectric spectroscopy, and switching time studies. We have also characterized the thermal stability, fatigue endurance and breakdown strength of these films and report a tremendous improvement in the performance of these blend devices compared to unblended ferroelectric devices.

2. Results and Discussion

2.1. Physical Characterization of Polymer Blend Films

2.1.1. Morphology

A schematic of the nanoscale phase-separated polymer blend devices is shown in **Figure 1**a. The active single-layer consists of a blend film spin-cast from a solution of ferroelectric P(VDF-TrFE) and insulating PPO from a common solvent: methyl ethyl ketone. The morphology of these blend films consists of phase separated nanospheres of amorphous PPO, embedded in a semicrystalline, ferroelectric P(VDF-TrFE) matrix. Typically polymers are in a high state of entropy due to their highly disordered nature. As a result, when two polymers are blended together, it is very difficult to obtain a stable solid solution. Hence, upon evaporation of a common solvent, the polymers tend to phase seprate and form unstable nanostructures. However, polymers with high miscibility in a common solvent and strongly correlated chains due to hydrogen bonding and dipole-dipole interactions can lead to stable nanoscale phase separation.[10,18] P(VDF-TrFE) and PPO are highly miscible in MEK and stable in a large range of compositions from 0 to 25 wt% of PPO content. Figure 1b shows clear homogenous solutions from 2 wt% to 8 wt%. Solutions with up to 25 wt% PPO were made (see the Supporting Information) and remained stable even after a few weeks. Figure 1a also shows the chemical structure of P(VDF-TrFE) and PPO. PPO, i.e., poly(p-phenylene oxide) is an aromatic polyether with oxygen connected to aromatic aryl groups. Ethers are slightly polar in nature as the C–O–C bond angle in the functional group is about 110 degrees, and the C–O dipole does not cancel out. The presence of two lone pairs of electrons on the oxygen atoms makes hydrogen bonding with water and other polar molecules possible. We believe hydrogen bonding between the electronegative oxygen in PPO and electropositive hydrogen in P(VDF-TrFE) and the electropositive hydrogen in the methyl group of PPO and electronegative fluorine in P(VDF-TrFE) leads to stable, repeatable nanoscale phase separation of the polymers.

The surface morphology and phase separation of 120 nm thick polymer blend films spun on Pt/Si substrates was characterized using AFM (as shown in **Figure 2**. Figure 2a shows the typical morphology of P(VDF-TrFE) thin films annealed

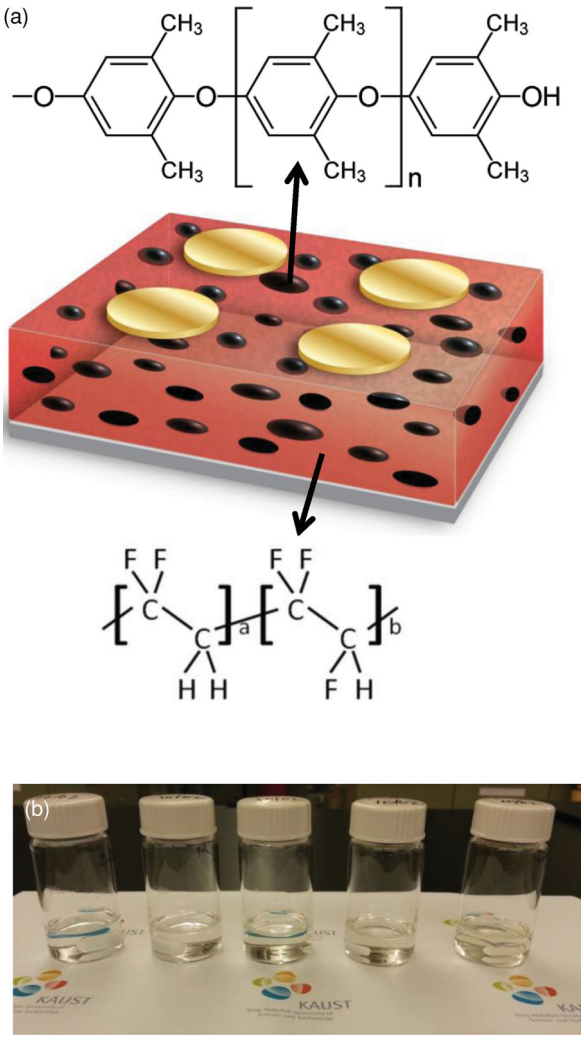

Figure 1. a) Schematic 3D cross section of ferroelectric capacitors with phase seperated blends of P(VDF-TrFE)–PPO sandwiched between Pt and Au electrodes. The morphology consists of phase separated nanospheres of amorphous PPO, surrounded by P(VDF-TrFE) matrix. b) Solutions with 0 wt%, 2 wt%, 4 wt%, 6 wt%, and 8 wt% PPO (left to right) showing clear, homogeneous, and stable solutions.

at 135 °C for 4 h, with crystalline grains about 80–100 nm in size. Figure 2b shows spun cast blend films with 6 wt% PPO, which was not subjected to any annealing process. The blends phase separate into amorphous PPO nanospheres (~140 nm in size) randomly distributed throughout the films surrounded by the semi crystalline P(VDF-TrFE) matrix. The AFM study confirmed that phase separation for these blends was spontaneous and not thermally stimulated. Figure 2c shows the phase image of the same blend film after annealing at 135 °C for 4 h. After annealing, we observe an increase in grain size of the semi crystalline P(VDF-TrFE) indicative of higher crystallinity but there is no significant change in the microstructure of PPO nanospheres or the roughness of the blend films. AFM measurements were performed as a function of blending ratio from 0 to 8 wt% PPO content. With increasing amount of PPO the average lateral size of PPO nanospheres increases

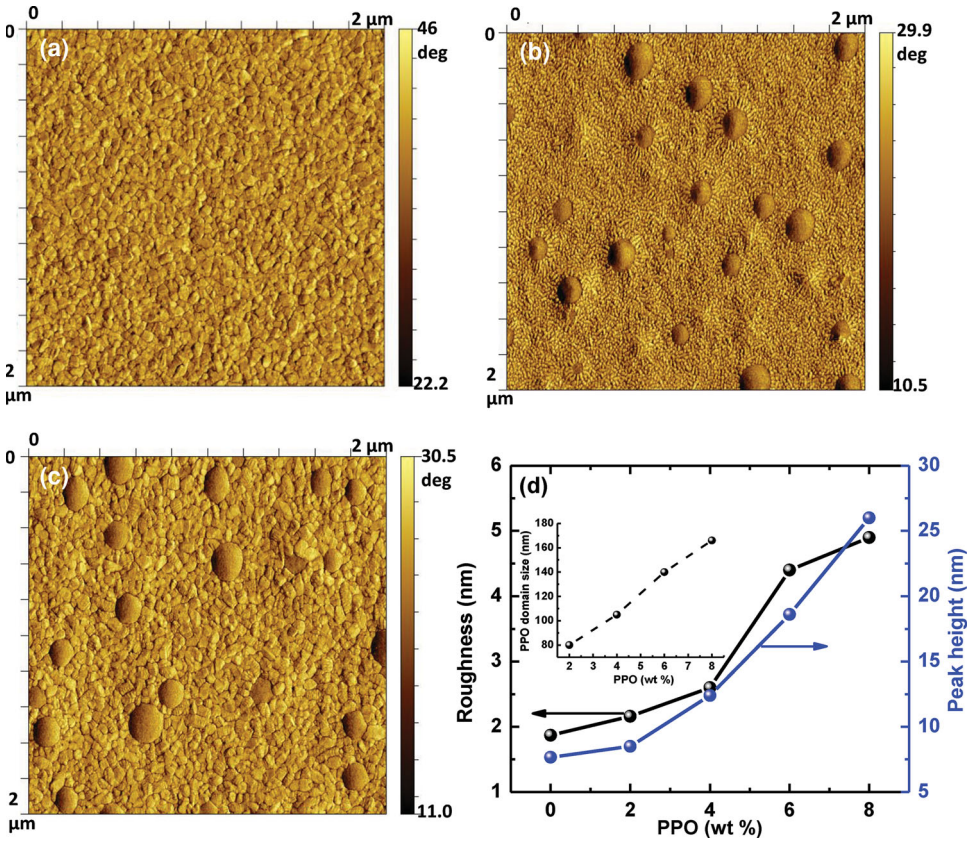

Figure 2. a) AFM phase image of pure P(VDF-TrFE) film showing island like grains in the film. b) AFM phase image of as spun blend films with 6 wt% PPO without annealing. c) AFM phase image of blend films with 6 wt% PPO after annealing at 135 °C, with increase in grain size of P(VDF-TrFE). d) R_{rms} (left) and peak height (right) of blend films as a function of PPO loading. The inset shows average size of the PPO nanospheres as calculated from the AFM phase images.

in a linear fashion from ~80 nm in a 2 wt% films, ~105 nm (4 wt%), ~140 nm (6 wt%), and ~165 nm for 8 wt% film as depicted in the inset of Figure 2d. This was calculated from the AFM phase images of blend films with different PPO loadings. Furthermore the number of PPO nanospheres decreases with increasing PPO content (see the Supporting Information), i.e., the phase separation coarsens with increasing PPO content. These observations seem to rule out that the solidification process is due to nucleation and growth. This leads us to believe that the phase separation might be due to spinodal decomposition in which the separation occurs uniformly throughout the film and not at distinct nucleation sites. Similar observation has been made for P(VDF-TrFE) blends with other polymers.[19] Spinodal decomposition can be contrasted with nucleation and growth. There the initial formation of the microscopic clusters involves a large free energy barrier, and so can be very slow, and may occur as little as once in the initial phase, not throughout the phase, as happens in spinodal decomposition. In the spinodal region there is no thermodynamic barrier to the reaction, thus the decomposition or phase separation is determined solely by diffusion.[19] Thus when dealing with polymer blends, various factors like their molecular weight, isotropy, temperature, composition, solvent properties etc. can affect the evolution and shape of the microstructures. From a practical standpoint, spinodal decomposition provides a means of producing a very finely dispersed microstructure that can significantly enhance the physical properties of the material.

The surface roughness of ferroelectric thin films is a very critical parameter when fabricating ferroelectric memory. High surface roughness leads to non-uniform electrical field across the active layer and possibly poor yield and reproducibility for ferroelectric capacitors and low mobility and low ON/OFF ratios in ferroelectric transistors.[2,19,20] The measured surface roughness from the topography images (see the Supporting Information) of these blend films annealed at 135 °C for 4 h, show relatively smooth films with an increase in roughness from ~2 nm for pure P(VDF-TrFE) films to ~5 nm for a blend film with 8 wt% PPO. As seen from Figure 2d, with increasing amounts of PPO the peak height of the amorphous PPO nanospheres increases hence leading to increase in roughness. This can be further optimized and improved using techniques like temperature assisted wire-bar coating which has recently been used to fabricate smooth, polymer blend thin films.[10,21]

The cross section morphology and phase separation was characterized through transmission electron microscopy (TEM) as seen in **Figure 3**. Figure 3a shows the cross section TEM image of a 120 nm thick pure P(VDF-TrFE) thin film. Figures 3b–d show the cross sections of 6 wt% PPO blend film

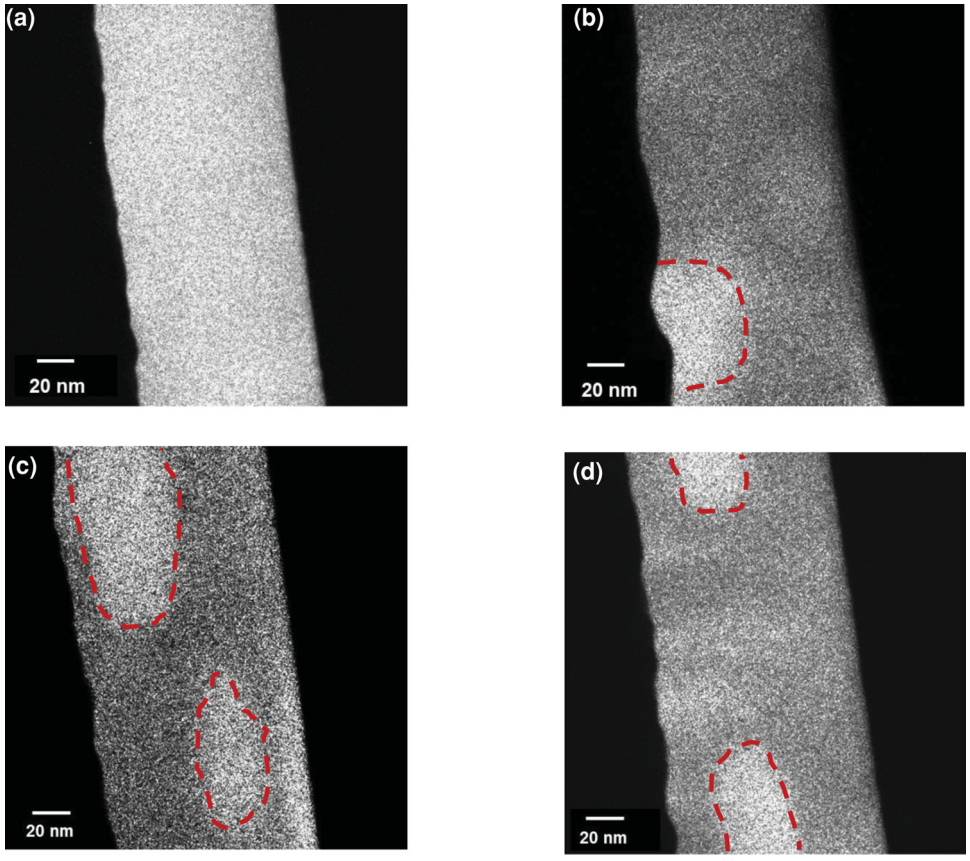

Figure 3. Cross section TEM images of pure P(VDF-TrFE) films (a) and blend films with 6 wt% PPO (b,c,d).

sandwiched between Pt and Au electrodes at different locations. The TEM images confirm the morphology of these blend films consists of phase separated nanospheres of amorphous PPO, surrounded by a ferroelectric P(VDF-TrFE) matrix as seen by AFM. The observed phase separation was seen in multiple locations throughout the film, as shown in Figure 3c and d.

2.1.2. Crystal Structure and Orientation

Figure 4a shows the Grazing Incidence X-ray diffraction (GIXRD) spectra which was used to study the crystal structure of pure ferroelectric P(VDF-TrFE) and the polymer blends with PPO. Pristine P(VDF-TrFE) films spun on Pt electrodes and annealed at 135 °C exhibit a peak centered at $2\theta \sim 19.78°$, characteristic of the ferroelectric β phase and reflection from the (110) and (200) planes.[1,22,23] The inter-planar distance was calculated to be approximately 4.48 Å and is consistent with earlier reports.[22,24] The broad peak is typical of a semicrystalline polymer like P(VDF-TrFE) comprising of crystalline lamella and amorphous regions. It is very important to have highly crystalline ferroelectric thin films as only the β-crystalline regions in the films give rise to ferroelectricity because the dipole moments in the amorphous regions will be random and cancel out each other.[2] X-ray diffraction is the primary technique to determine crystallinity of semicrystalline polymers and has been previously used for P(VDF-TrFE) thin films.[23] The determination of the degree of crystallinity implies use of a two-phase model, i.e., the sample is composed of crystalline and amorphous regions, and no regions of semi-crystalline organization. The diffraction peak observed could be well resolved into two peaks, C (Crystalline) and NC (Non crystalline). We used a gaussian function to get the best fitting. The degree of crystallinity can be caluclated from the ratio of area under C to total area under C+N. The calcualted degree of crystallinity for pure P(VDF-TrFE) was ~74%, typical of very thin (~100–200 nm) P(VDF-TrFE) films.[25] Figure 4b shows the XRD peak for blend films with 8% PPO content. The blend films with PPO exhibit a peak slightly shifted to the right at $2\theta \sim 19.9°$ for 8 wt% PPO films, indicating a slightly smaller polymer chain inter-planar distance of ~4.45 A°. More importantly we noticed lower crystallinity for blend films with increasing PPO content, and was ~62% for 8 wt% PPO films. This is typical for blend films and has been observed for P(VDF-TrFE)-PMMA blend systems as well.[11,26]

The presence of PPO in thin films of the polymer blend was verified using transmission mode Fourier transform infrared (FTIR) spectroscopy. Figure 4b shows the absorbance bands at 1288 cm^{-1} and 850 cm^{-1} associated with CF_2 symmetric stretching vibration and are characteristic bands of the trans-zigzag formation (β phase).[22,27,28] Other major peaks identified are the 1400 cm^{-1} band characteristic of the CH_2 wagging vibrations, 1186 cm^{-1} band characteristic of asymmetric stretching of CF_2 and the 880 cm^{-1} band related to the rocking CH_2 vibration.[22,27,28] All these peaks were common in both

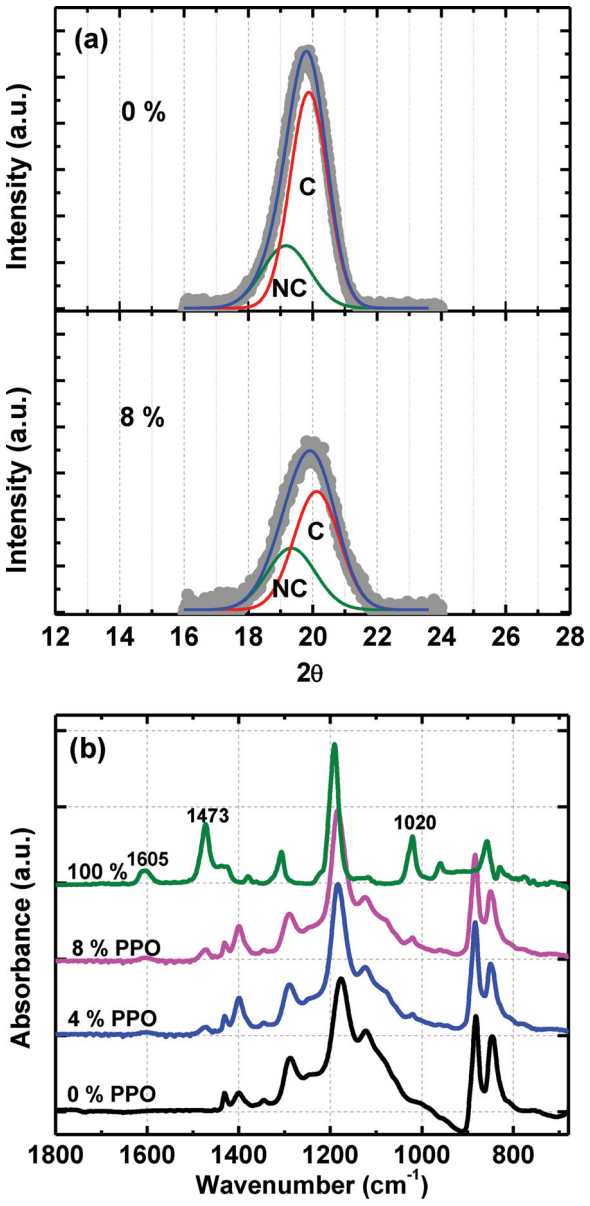

Figure 4. a) Grazing incidence XRD spectra for pure ferroelectric P(VDF-TrFE) films and blend films with 8 wt% PPO. b) FT-IR spectra of pure ferroelectric P(VDF-TrFE) thin film, pure PPO thin film and blend films with 4 wt% and 8 wt% PPO.

pristine P(VDF-TrFE) and P(VDF-TrFE)-PPO blended films. A few additional peaks were identified in the blend films at 1605 cm^{-1} characteristic of C–C=C symmetric stretching in the benzene ring, 1473 cm^{-1} from C–C=C asymmetric stretching and 1020 cm^{-1} from C–O stretching confirming the presence of functional ether group in PPO.[17,29,30] It is important to mention here that we could not detect the methyl fucntional groups in FTIR spectra which might be due to overlapping with other peaks or due to the poor resolution of the FTIR equipment. FTIR analysis proves the presence of PPO in these polymer blend films, but does not suggest any interaction or bonding between the PPO and P(VDF-TrFE) chains.

2.2. Ferroelectric and Dielectric Performance of Blend Films

Figure 5a shows the polarization-electric field hysteresis loops for P(VDF-TrFE)-PPO blend devices. The devices measured at 10 Hz exhibit well-saturated hysteresis curves and pure P(VDF-TrFE) capacitors show a remnant polarization ($\pm P_r$) of 7.3 $\mu C/cm^2$ and coercive field of ~62 ± 5 MV/m. With increasing PPO content, a monotonic decrease in remnant polarization and increase in coercive fields is observed. Blend films with 8 wt% PPO exhibit a remnant polarization ($\pm P_r$) of 4.93 $\mu C/cm^2$ and coercive field of ~67 ± 5 MV/m. This effect can be attributed to the decrease in crystallinity of the films upon adding PPO, as seen from the X-ray diffraction peaks in Figure 4a.

In ferroelectric capacitors, it is critical that the difference between switching and non-switching current is maximized to be able to distinguish the "0" from "1" memory state. Figure 5b shows that with increasing PPO content the switching current gradually decreases. But even with high amounts of PPO content upto 8 wt%, our blend capacitors display good switching current density ~ 15 $\mu A/cm^{2;}$ comparable to reports of pure P(VDF-TrFE) based ferreoelctric capacitors.[31,32] At the same time we measured the switching time characteristics of our P(VDF-TrFE)-PPO blend films, which can be obtained by a time domain measurement of the charge density or polarization (P) response. Switching times (τ_s) are estimated from the time of the maximum of dP/d(logt) vs. log (t) plot and are plotted in the inset of Figure 5b.[33] At applied fields of 125 MV/m, pure P(VDF-TrFE) capacitors devices exhibit switching times of 0.19 ms while devices with 8 wt% PPO have similar switching times of ~0.21 ms. Thus switching times do not vary significantly with increase in PPO content, another important requirement for ferroelectric memories.

One of the biggest advantages of using PVDF-based ferroelectric polymers is their high permittivity, which comes from their ability to polarize under an applied electric field. This makes it possible to fabricate devices with low operating voltages using them as a dielectric layer. A gate dielectric with high permittivity reduces the operating voltage of OTFTs effectively without the need for thickness reduction.[26] Thus, it is important to characterize the effect of PPO on dielectric dispersion of these blend films. Figure 5c shows the dielectric dispersion and the loss factor (tan δ) of pure P(VDF-TrFE), pure PPO and blend ferroelectric capacitors. Our P(VDF-TrFE) copolymer films exhibit a dielectric constant of ~11 at 100 Hz, comparable to other reports in literature.[34] A gradual decay of the dielectric permittivity (ε_r) is observed for pure P(VDF-TrFE) capacitors, consistent with the dielectric response of a polar polymer dielectric where the dipoles cannot respond to the applied field at high frequencies. On the other hand PPO exhibits a dielectric constant of ~3 and a dielectric response which is independent of frequency, typical of low dielectric constant polymer dielectrics. In such materials the electronic polarization is the major contributor to the overall permittivity and its response to the frequency of the applied field is almost instantaneous. Figure 5c also shows the dielectric dispersion of our blend capacitors. With increasing amounts of PPO, the permittivity gradually drops but is relatively high for low voltage electronic applications; an 8 wt% blend film has a ε_r ~ 9.3. Figure 5c also shows the dielectric losses (tan δ) calculated

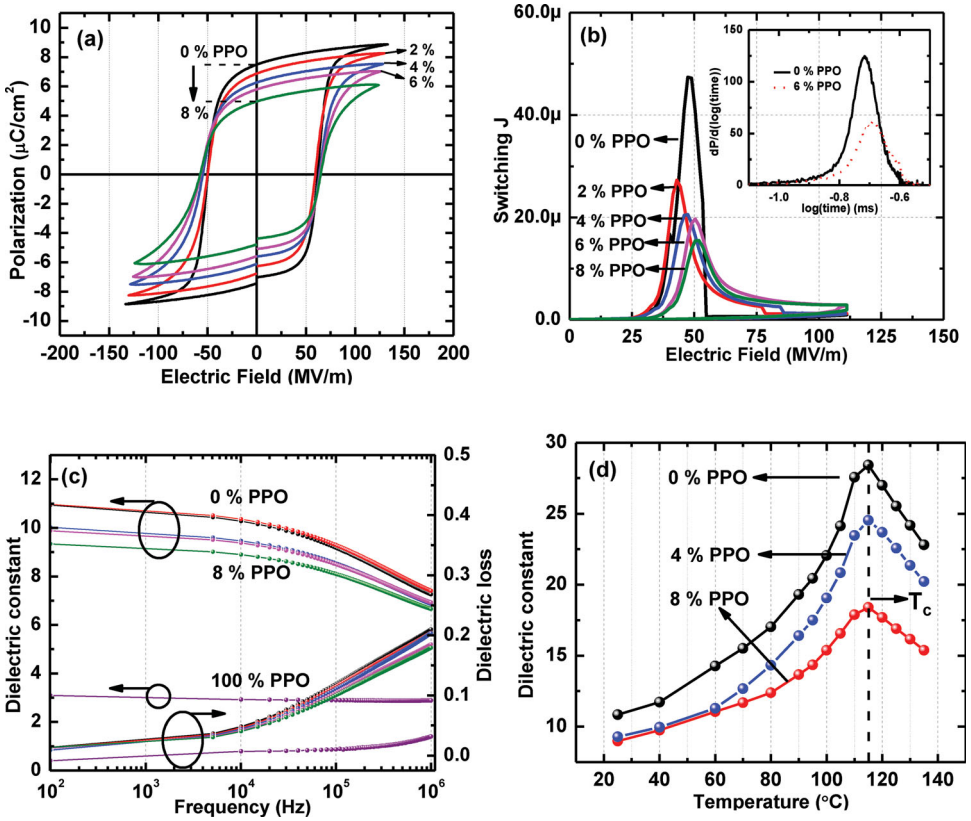

Figure 5. a) Polarization–electric field hysteresis loop measurements for blend films at 10 Hz as a function of amount of PPO. b) Switching current response from blend films with 0 to 8 wt% PPO and with platinum/gold electrodes. The inset shows switching characteristics for blend film at 125 MV/m, with peak of dP/d(log(t)) vs. log(t) representing respective switching times. c) Dielectric spectroscopy study with dielectric constant (left axis) and dielectric losses (right axis) for blend films with 0 to 8 wt% PPO and pure PPO films. d) Temperature dependance of dielectric permittivity for devices with 0, 4, and 8 wt% PPO at 1 KHz.

from the ratio of the imaginary and real part of the dielectric constant indicating power dissipation from the dielectric layer. An ideal dielectric should have high permittivity and low losses for electronic applications. Our blend films with 8 wt% PPO show lower dielectric losses (0.17 at 1 MHz) compared with the baseline pure P(VDF-TrFE) films (0.21 at 1 MHz) resulting from the excellent insulating and low power dissipation properties of the PPO phase. Thus with small amounts of PPO, it is possible to maintain relatively high permittivity in the blend films and at the same time lower the dielectric losses.

Figure 5d shows the temperature dependence of the dielectric permittivity of our blend films. The dielectric permittivity of our ferroelectric capacitors increases with temperature, reaches a maximum, then decreases. This behavior is typical of ferroelectric materials which when subjected to heating–cooling cycle undergo a ferroelectric-to-paraelectric phase transition at the Curie temperature (T_c). The curie temperature for our pure P(VDF-TrFE) films is approx. ~115 °C, consistent with reports in literature.[24,35] Interestingly blend films with increasing amount of PPO don't show any change curie temperature. This is typical of phase separated thin films and has been observed for P(VDF-TrFE) and PMMA blend system as well.[11,14]

2.3. Thermal Stability of Blend Films

Large scale integration of ferroelectric memory based on the copolymer P(VDF-TrFE) remians a big challenge due to its poor thermal stability.[3] We have studied the thermal stability of our pure P(VDF-TrFE) and blend capacitors with 8 wt% PPO content. The devices were evaluated based on their ability to switch polarization at an applied field of 125 MV/m and a frequency of 10 Hz. **Figure 6**a shows the measured remnant polarization and coercive field vs. temperature. In general, a slight increase in polarization and decrease in coercive field is observed with increasing temperature, since the elevated temperatures supply some of the required energy to switch the dipoles.[36] Thermal stability of PVDF and PVDF based ferroelectric polymers is directly related to their Curie temperature as these polymer undergo a ferroelectric-paraelectric transition at the Curie temperature.[24] Interstingly, we noticed a rapid deterioration in stability of our pure P(VDF-TrFE) thin film capacitors at only 50 °C. This is consistent with other reports for thin film P(VDF-TrFE) capacitrors that the polarization decreases notably at 50 °C and rapidly deteriorates at even higher temperatures.[3] This was suprising as it is still way below the curie temperature of ~110–120 °C for a 70/30 molar ratio copolymer.[35,36] In contrast, blend films with 8 wt% PPO, showed much better thermal

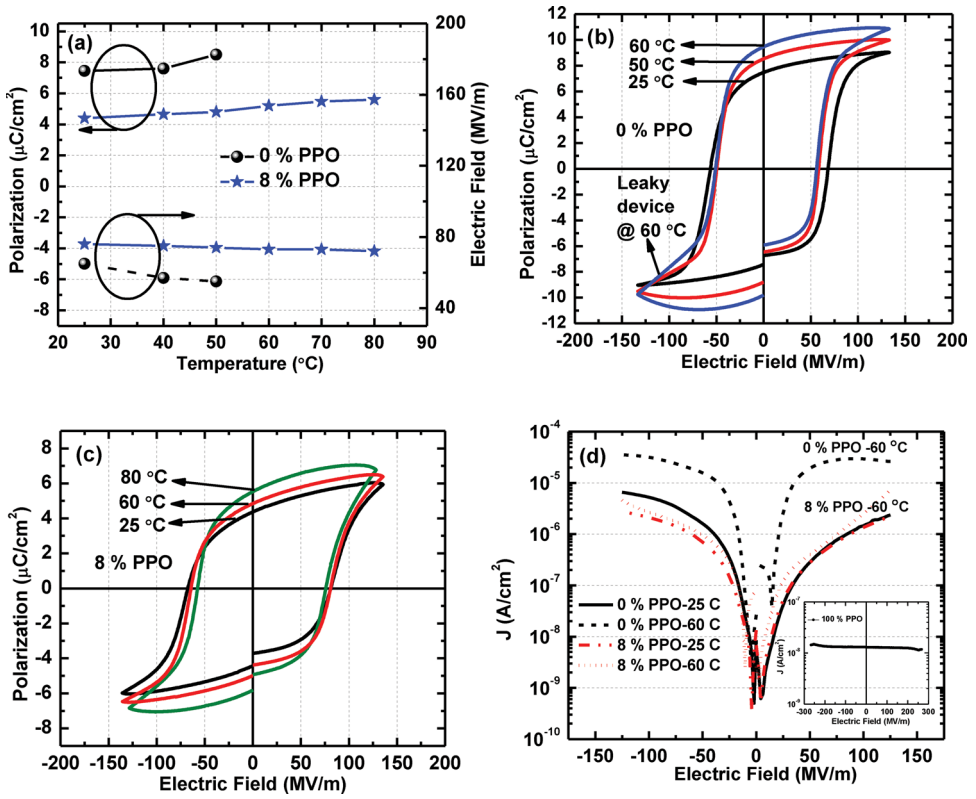

Figure 6. a) Remnant polarization and coercive field as a function of temperature for pure P(VDF-TrFE) films and blend films with 8 wt% PPO. b) Polarization–electric field hysteresis loop measurements for pure P(VDF-TrFE) films at 10 Hz as a function of temperature. c) Polarization–electric field hysteresis loop measurements for blend films with 8 wt% PPO at 10 Hz as a function of temperature. d) Current density–electric field measurements of blend films (0, 8 wt% PPO) at 0 °C and 60 °C. A voltage of approximately 15 (125 MV/m) was applied to pole the devices before measuring the leakage current in the devices. The inset shows the leakage current density of pure PPO device with Pt/Au electrodes.

stability compared to pure P(VDF-TrFE) capacitors. The devices perform well upto 80 °C which are closer to curie temperature of the copolymer. The improvement in thermal stability cannot come from change or increase in curie temperature of the blend films as seen in Figure 5d. Figure 6b show the hysteresis loops for pure P(VDF-TrFE) capacitors at different temperatures. We observed that at temperatures of 60 °C or above, the hysteresis loops displayed a resistive leaky behavior making it impossible to accurately determine polarization in these films. At higher temperatures we noticed very leaky curves especially in the negative bias regime, indicative of surface breakdown at one of the electrode/ferroelectric interfaces. In contrast, the blend films with PPO show better saturated curves at high temperatures as shown in Figure 6c.

To further understand this we studied the leakage current of pure P(VDF-TrFE) films and blend films as a function of temperature. Leakage of ferroelectric capacitors based on the copolymer has been well studied and shows a relatively high leakage for thin films around 100 nm.[22,37] The introduction of TrFE is very effective in obtaining the ferroelectric β phase in the copolymer but also leads to larger leakage current. Figure 6d shows that at saturation fields of ~125 MV/m pure P(VDF-TrFE) capacitors show leakage current density in excess of 10^{-6} A/cm^2 at room temperature. On the other hand pure PPO films display low leakage crurrent of ~10^{-8} A/cm^2 even at high fields ~300 MV/m further highlighting the excellent insulating properties of PPO. The blend devices with 8 wt% PPO show similar leakage currents with sligthly lower currents on the negative bias. We believe its because of current conduction through the more leaky majority ferroelectric phase. More importantly what we noticed a drastic improvement in leakage current of the blend films compared to pristine P(VDF-TrFE) films at higher temperatures of 60 °C. This leakage current density of the blend films does not change much with temperature and is an order of magnitude lower than P(VDF-TrFE) films at 60 °C. We believe that the highly insulating amorphous nanospheres of PPO in the blend films acts as good charge trap regions and do not allow charge carriers to move freely through the film. This directly affects thermal stability of these blend films leading us to reliably switch the polarization even at elevated temperatures.

2.4. Fatigue Endurance and Breakdown Strength of Blend Films

Polarization fatigue is the reduction of amount of switchable polarization with repeated switching cycles and still remains an elusive problem for the ferroelectric copolymer. The fatigue characterization of the copolymer is rather complicated since it depends on many parameters such as the

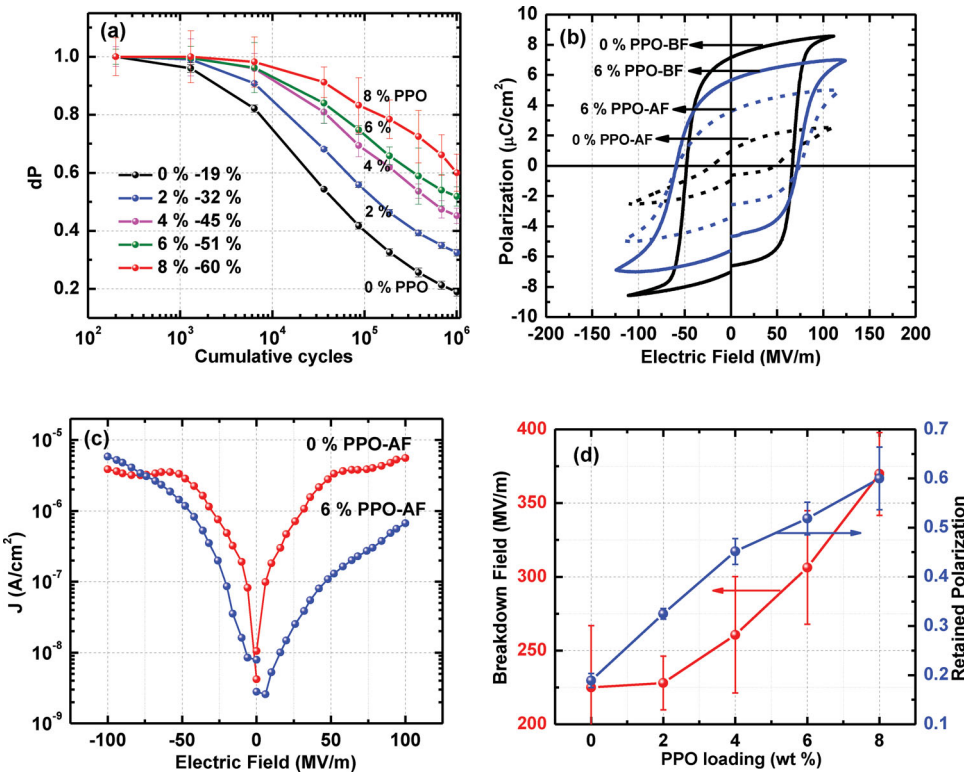

Figure 7. a) Electrical fatigue properties showing relative polarization of blend films with 0 to 8 wt% PPO. The films were stressed at 100 MV/m and a frequency of 100 Hz and the PUND measurements were done at saturation fields of 125 MV/m and 100 Hz. b) Polarization–electric field hysteresis loop measurements for pure P(VDF-TrFE) films and 6 wt% PPO films before (BF) and after fatigue (AF), characterized also at 100 Hz. c) Current density–electric field measurements of pure P(VDF-TrFE) films and 6 wt% PPO films after fatigue upto 10^6 cycles at 100 Hz. d) Dielectric breakdown strength (left) and Fatigue or polarization retention after 10^6 cycles (right) as a function of amount of PPO in blend films.

thickness of film, molar ratio of the copolymer, frequency of stress waveform,applied field, temperature and electrodes of the capacitor.[5] Here we report the fatigue performance of our capacitors with common Pt and Au electrodes under relevant and correct conditions.[5,8] **Figure 7**a shows the fatigue performance of our P(VDF-TrFE)-PPO blend film capacitors upto a million (10^6) cycles. A bipolar triangular waveform with an electric field of 100 MV/m and 10 ms pulse width (100 Hz) was applied to fatigue the devices. The polarization was characterized periodically with a positive-up-negative-down (PUND) measurement at 125 MV/m at the same frequency. We observed a gradual improvement in the fatigue performance of our blend devices with increasing PPO content. With approx. 8 wt% PPO, the devices retain ~60% of the polarization after 10^6 cycles, which is a tremendous improvement from pure P(VDF-TrFE) capacitors which only retain ~20% of the polarization. Figure 7b shows the hysteresis curves at 100 Hz measured before and after fatigue cycles. We can see that the polarization decreases sharply from ~7 μC/cm^2 to only 1 μC/cm^2 for pure P(VDF-TrFE), while for 6 wt% PPO films the polarizations drops marginally from ~5.6 μC/cm^2 to ~3.6 μC/cm^2. The devices were also fatigued at a higher frequency of 1 kHz which is close to the maximum frequency at which we can switch the polarization of our copolymer films. Even at higher frequencies the films with 8 wt% PPO show excellent polarization retention of ~80% after 10^6 cycles compared to 54% for pure P(VDF-TrFE) films (see the Supporting Information). The frequency dependence of fatigue performance for ferroelectric memory has been well studied before with devices showing better fatigue performance at higher frequencies.[5] It has been proposed that fatigue in P(VDF-TrFE) film is related to the injection of charges from electrodes which are subsequently trapped at crystallite boundaries and defects, inhibiting ferroelectric switching and leading to higher fatigue rates.[5,8] To further understand the fatigue mechanism we compared the current-voltage (leakage) characteristics of the pure and blend film devices after fatigue. Figure 7c shows high leakage current through fatigued P(VDF-TrFE) film while the films with 6 wt% PPO content show much lower leakage after fatigue. This suggests that the high number of trapped charges in pure P(VDF-TrFE) films causes poor fatigue performance. The leakage current of the P(VDF-TrFE) thin films also shows an S shaped behavior at high fields,exhibiting small negative differential resistance. This phenomena has been well observed in breakdown studies of polymer dielectrics.[38] This indicates current instability in the film; a situation in which a homogeneous current distribution becomes unstable and decays into filaments.[38] The local charge and current densities are larger; leading to electrical thinning of the film. This is the reason for the lower coercive fields seen for our films after fatigue (Figure 7b). This can also lead to a vastly increased thermal stress leading to electrode delamination also reported in literature especially with the use of unreactive metals such

as Au.[36] We have also observed this during the fatigue of our pure P(VDF-TrFE) capacitors, where in some devices the top Au electrode delaminates due to the high thermal stress (see the Supporting Information). Thus continous fatigue of thin film P(VDF-TrFE) ferroelectric capacitors leads to dielectric aging and a film close to breakdown. In contrast, blend films with PPO show only a slight increase in leakage current after fatigue, due to the good insulating and charge trapping properties of the PPO nanospheres which results in better fatigue endurance. These highly insulating nanospheres in the blend films act as good charge trap regions and do not allow charges to get trapped in the ferroelectric film, thereby improving fatigue performance. In a follow up study we also measured the dielectric breakdown strength of the blend films. Dielectric breakdown strength using short time tests where the sweeping DC voltage was applied at a ramp rate of 3 V/s to reach device failure between 10–20 s was performed. Figure 7d shows that with increasing PPO content, the breakdown strength of these films improves from ~225 MV/m to ~360 MV/m for 0% PPO to 8 wt% PPO content, respectively.[39] The PPO in the blend films with its good insulating properties as well as its inherently high dielectric breakdown strength helps improve the breakdown strength of these P(VDF-TrFE)-PPO blend ferroelectric memory devices.

3. Conclusion

We have fabricated ferroelectric memory from polymer blends consisting of phase-separated ferroelectric P(VDF-TrFE) and highly insulating amorphous Polyphenylene oxide (PPO). The morphology of these blend films consists of phase separated nanospheres of amorphous PPO, surrounded by a crystalline ferroelectric P(VDF-TrFE) matrix. The highly insulating amorphous nanospheres of PPO in the blend films acts as good charge trap regions and do not allow charge carriers to move freely through the film. This directly affects the ferroelectric and dielectric performance of the devices. The blend devices display highly improved ferroelectric and dielectric performance with low dielectric losses (<0.2 up to 1MHz), enhanced thermal stability (~up to 353 K), excellent fatigue endurance (80% retention after 10^6 cycles at 1 KHz) and high dielectric breakdown fields (~360 MV/m). The blend devices provide a solution to some of the important limitations of ferroelectric memory based on the copolymer, making ferroelectric memory devices based on these blends more suitable for flexible and transparent electronic applications.

4. Experimental Section

Sample Preparation: The polymer blend thin films were fabricated on Platinum coated silicon substrates. Prior to device fabrication, the substrates were cleaned by ultra-sonication in acetone, isopropanol, and DI water. P(VDF-TrFE) (70/30 mol%) obtained from Piezotech S.A, France was dissolved in anhydrous Methyl Ethyl Ketone (MEK) at a concentration of 20 mg/mL to make a 2 wt% solution. High purity low molecular weight polyphenylene oxide (Noryl SA90 PPO) (M_n~1800) obtained from Saudi Basic Industries Corporation (SABIC) was dissolved in 10 mL P(VDF-TrFE) solutions by varying the amounts (4.08 mg, 8.22 mg, 12.76mg, 17.39 mg, 27.27 mg) to make 2 wt% to 8 wt% P(VDF-TrFE)-PPO blend solutions. All the different concentrations of PPO formed clear homogenous solutions stable even after a few weeks. The filtered polymer blend films were spun in a nitrogen filled glove box, at 4000 rpm for 60 s followed by a soft bake for 20 min at 70 °C. The films were then annealed in vacuum at 135 °C for 4 h to improve the crystallinity of the P(VDF-TrFE) phase. The thickness of the blend films was ~120 ± 10 nm as measured by a Dektak profilometer, and did not change much with increasing PPO concentrations. To complete the device, ~80 nm Gold was thermally evaporated through a shadow mask to define the top electrodes.

Characterization: All current–voltage measurements were carried out in air ambient using Keithley 4200 semiconductor characterization system, while Polarization-Voltage and fatigue tests were done using the Premier Precision II ferroelectric tester (Radiant Technologies Inc.). Surface morphology and roughness for the blend films was studied using Atomic Force Microscopy (Agilent 5400). Cross section morphology of the devices was studied using Transmission Electron Microscopy (Titan ST) and operated at an accelerating voltage of 300 kV. Energy Filtered TEM analysis was done to elementally map carbon in the polymer blend films. The crystallinity and inter-planar spacing of polymer chains was evaluated using Grazing Incidence X-ray Diffraction (Bruker D8 Discover) while the bonding and dipole orientation was analyzed using Fourier-transform infrared spectroscopy (FT-IR, ThermoScientific Nicolet iS10).

Supporting Information

Supporting Information is available from the Wiley Online Library or from the author.

Acknowledgements

The authors acknowledge the generous financial support from KAUST and Saudi Basic Industries Corporation (SABIC) Grant No. 2000000015.

Received: June 16, 2013
Revised: August 22, 2013
Published online: October 29, 2013

[1] Y. J. Park, I.-S. Bae, S. J. Kang, J. Chang, C. Park, *IEEE. T. Dielect. El. In.* **2010**, *17*, 1135.
[2] R. C. G. Naber, K. Asadi, P. W. M. Blom, D. M. de Leeuw, B. de Boer, *Adv. Mater.* **2010**, *22*, 933.
[3] M. Li, H. J. Wondergem, M.-J. Spijkman, K. Asadi, I. Katsouras, P. M. Blom, D. M. d. Leeuw, *Nat. Mater.* **2013**, 1.
[4] S. Horie, K. Ishida, S. Kuwajima, K. Kobayashi, H. Yamada, K. Matsushige, *Jpn. J. Appl. Phys.* **2008**, *47*, 1259.
[5] G.-D. Zhu, X.-Y. Luo, J.-H. Zhang, Y. Gu, *IEEE. T. Dielect. El. In.* **2010**, *17*, 1172.
[6] H. Xu, J. Zhong, X. Liu, J. Chen, D. Shen, *Appl. Phys. Lett.* **2007**, *90*, 092903.
[7] S. Z. Yuan, X. J. Meng, J. L. Sun, Y. F. Cui, J. L. Wang, L. Tian, J. H. Chu, *Phys. Lett. A* **2011**, *375*, 1612.
[8] G. Zhu, Y. Gu, H. Yu, S. Fu, Y. Jiang, *J. Appl. Phys.* **2011**, *110*, 024109.
[9] Q. Chen, B. Chu, X. Zhou, Q. M. Zhang, *Appl. Phys. Lett.* **2007**, *91*, 062907.
[10] M. Li, N. Stingelin, J. J. Michels, M.-J. Spijkman, K. Asadi, K. Feldman, P. W. M. Blom, D. M. de Leeuw, *Macromolecules* **2012**, *45*, 7477.
[11] R. L. Moreira, L. O. Faria, G. Marini, C. Wisniewski, J. A. Giacometti, *Ferroelectrics* **2002**, *268*, 101.

[12] S. J. Kang, Y. J. Park, I. Bae, K. J. Kim, H.-C. Kim, S. Bauer, E. L. Thomas, C. Park, *Adv. Funct. Mater.* **2009**, *19*, 2812.
[13] I. Bae, S. J. Kang, Y. J. Park, T. Furukawa, C. Park, *Curr. Appl. Phys.* **2010**, *10*, 54.
[14] L. O. Faria, R. L. Moreira, *J. Polym. Sci. Pol. Phys.* **1999**, *37*, 2996.
[15] J.-W. Yoon, S.-M. Yoon, H. Ishiwara, *Jpn. J. Appl. Phys.* **2010**, *49*, 030201.
[16] B. X. Du, H. J. Liu, X. H. Wangl, X. Zhang, *Proc. 9th Int. Conf. Properties Appl. Dielect. Mater.* **2009**, 565.
[17] S. B. Gajbhiye, *Int. J. Modern Engin. Res.* **2012**, *2*, 941.
[18] L. Zhang, *Europhys. Lett.* **2011**, *93*.
[19] K. Asadi, H. J. Wondergem, R. S. Moghaddam, C. R. McNeill, N. Stingelin, B. Noheda, P. W. M. Blom, D. M. de Leeuw, *Adv. Funct. Mater.* **2011**, *21*, 1887.
[20] M. A. Khan, U. S. Bhansali, D. Cha, H. N. Alshareef, *Adv. Funct. Mater.* **2012**, *23*, 2145.
[21] M. Li, N. Stingelin, J. J. Michels, M.-J. Spijkman, K. Asadi, R. Beerends, F. Biscarini, P. W. M. Blom, D. M. de Leeuw, *Adv. Funct. Mater.* **2012**, *22*, 2750.
[22] M. A. Khan, U. S. Bhansali, H. N. Alshareef, *Org. Electron.* **2011**, *12*, 2225.
[23] Y. Tajitsu, H. Ogura, A. Chiba, T. Furukawa, *Jpn. J. Appl. Phys.* **1987**, *26*, 554.
[24] U. S. Bhansali, M. A. Khan, H. N. Alshareef, *Org. Electron.* **2012**, *13*, 1541.
[25] Z.-G. Zeng, G.-D. Zhu, L. Zhang, X.-J. Yan, *Chinese. J. Polym. Sci.* **2009**, *27*, 479–485.
[26] S.-W. Jung, K.-J. Baeg, S.-M. Yoon, I.-K. You, J.-K. Lee, Y.-S. Kim, Y.-Y. Noh, *J. Appl. Phys.* **2010**, *108*, 102810.
[27] A. A. Prabu, K. J. Kim, C. Park, *Vib. Spectrosc.* **2009**, *49*, 101.
[28] N. M. Reynolds, K. J. Kim, C. Chang, S. L. Hsu, *Macromolecules* **1989**, *22* 1092.
[29] B. C. Kim, S. Nair, J. Kim, J. H. Kwak, J. W. Grate, S. H. Kim, M. B. Gu, *Nanotechnology* **2005**, *16*, S382.
[30] N. Shimizu, Y. Kuwahara, *Biosci. Biotechnol. Biochem.* **2001**, *65*, 990.
[31] K. H. Lee, G. Lee, K. Lee, M. S. Oh, S. Im, *Appl. Phys. Lett.* **2009**, *94*, 093304.
[32] S. H. Noh, W. Choi, M. S. Oh, D. K. Hwang, K. Lee, S. Im, S. Jang, E. Kim, *Appl. Phys. Lett.* **2007**, *90*, 253504.
[33] T. Furukawa, T. Nakajima, Y. Takahashi, *IEEE. T. Dielect. El. In.* **2006**, *13*, 1120.
[34] M. A. Khan, U. S. Bhansali, X. X. Zhang, M. M. Saleh, I. Odeh, H. N. Alshareef, *Appl. Phys. Lett.* **2012**, *101*, 143303.
[35] S. Ducharme, A. V. Bune, V. M. Fridkin, L. M. Blinov, S. P. Palto, A. V. Sorokin, S. G. Yudin, A. Zlatkin, *Nature* **1998**, *391*, 874.
[36] X. Zhang, H. Xu, Y. Zhang, *J. Phys. D. Appl. Phys.* **2011**, *44*, 155501.
[37] S. Fujisaki, H. Ishiwara, Y. Fujisaki, *Appl. Phys. Lett.* **2007**, *90*, 162902.
[38] H. R. Zeller, *IEEE. T. Electr. Insul.* **1987**, *22*, 115.
[39] M. N. Almadhoun, U. S. Bhansali, H. N. Alshareef, *J. Mater. Chem.* **2012**, *22*, 11196.